This paper first appeared in the tenth print edition of *Photovoltaics International* journal, published in November 2010.

Fabrication of single diffusion step selective-emitter solar cells

Ching-Hsi Lin[1], **Chien-Hua Lung**[1], **Yang-Fang Chen**[2,3], **Yu-Wei Tai**[2] and **Wei-Chih Hsu**[1],
[1]ITRI/Green Energy & Environment Research Labs, Hsinchu, Taiwan
[2]Neo Solar Power Corporation, Hsinchu, Taiwan
[3]National Taiwan University/Department of Physics, Taipei, Taiwan

ABSTRACT

A selective emitter is a doping layer that is heavily doped beneath the electrode and lightly doped in between the electrode grids. One of the disadvantages of conventional selective-emitter techniques is the need for a high phosphorus surface concentration to obtain low contact resistance and limit the shunts in the emitter. Effective emitter passivation below the contact is difficult because of the use of emitters with low sheet resistances and high doping concentrations. In this study, the selective emitter in the optimized light/light sheet-resistance combination was formed to reduce recombination under the metal contact. The fabrication of optimized light/light doped emitters was performed using a single-step diffusion process. Besides the benefit of low surface recombination for light/light combination, this approach also removes the need for a very precise alignment between the opened emitter pattern and the front screen-printed silver fingers. This work illustrates the achievement of an efficiency improvement of more than 0.4% absolute in large-scale production for selective emitter solar cells.

Introduction

Energy production using solar cells is a promising market. It is anticipated that crystalline silicon solar cells will contribute to the widespread adoption of photovoltaic applications as the primary photovoltaic technology. As research is conducted worldwide in the search for methods of improving cell efficiencies and/or reducing costs, the next few decades should see the industry become cost competitive with its fossil fuel counterpart in many parts of the world.

Further expansion of the solar cell industry will require significant cost reduction. The cost of the solar cell can be reduced by either lowering the processing fee or by further enhancing the cells' conversion efficiency while controlling expenditure. The manufacture of industrial solar cells demands the development of new solar cell structures in order to reach higher efficiencies. Successful implementation of new

technologies into the cell manufacturing industry will require a keen eye on the costs involved in incorporating these techniques. This study succeeded in developing a cost-effective selective-emitter technique through a single diffusion step.

> "The manufacture of industrial solar cells demands the development of new solar cell structures in order to reach higher efficiencies."

A conventional commercial solar cell has a homogeneous emitter, which is usually formed by $POCl_3$ diffusion. An optimal emitter should have a high lateral conductivity and a low contact resistance which implies a high doping level. This, however, can induce severe Auger recombination and thus result in poorer spectral response. To achieve a high conversion efficiency, a compromise must be reached in the doping step. The other possibility is the concept of the selective emitter. A selective emitter is a doping layer that is heavily doped underneath the electrode and lightly doped between the electrode grids. Therefore, the illuminated areas are covered by a lowly-doped emitter layer. The advantages of a selective-emitter solar cell include a better short-wavelength response due to the low surface doping concentration, and a low contact resistance due to the heavy doping underneath the metal grid.

Selective emitter methodologies are of interest from the point of view of research, and tend to attract much attention throughout the photovoltaic industry. Various methods of formation of a selective-emitter on standard crystalline silicon solar cells have been developed [1-11]. Selective-emitter solar cells are usually fabricated via diffusion masking and subsequent pattern opening. There are several methods of opening the diffusion mask by use of laser ablation and application of etching paste. Ordinarily, this approach requires additional process steps compared to standard solar cell processes.

To successfully incorporate the selective-emitter technique into production, one of the requirements is that the efficiency of a selective emitter should be increased significantly compared to those conventional solar cells with uniformly-doped emitters. However, well-developed Ag pastes may limit the demand of selective-emitter techniques. The rapid developments of commercial front-side Ag pastes, which are suitable for high sheet-resistance silicon, make uniform lightly-doped solar cells possible. It is therefore necessary to develop a simple way of enhancing the efficiency at a low cost. In this study, we obtain low cost selective-emitter silicon solar cells through applying an optimized single diffusion step.

In conventional emitter cell constructs, a highly-doped emitter is present under the finger contacts, which makes effective emitter passivation below the contact quite difficult. A compromise must be arrived at between low recombination and low contact resistance. To reduce recombination under the metal contact, we implemented an effective light doping zone in the finger region. In addition, this paper explores the influences of various heavy/light doping combinations on the performance of multicrystalline silicon (mc-Si) selective-emitter solar cells. In comparison to mc-Si solar cells with a uniformly-doped 70Ω/sq emitter, an efficiency improvement of more than 0.4% absolute is achieved for selective-emitter solar cells. The selective-emitter structure was performed using a single diffusion step. Phosphorus was diffused through silicon oxide, which serves as a semi-transparent barrier. The wide lightly-doped region under the electrode removes the necessity of a very precisely-aligned Ag paste in this instance.

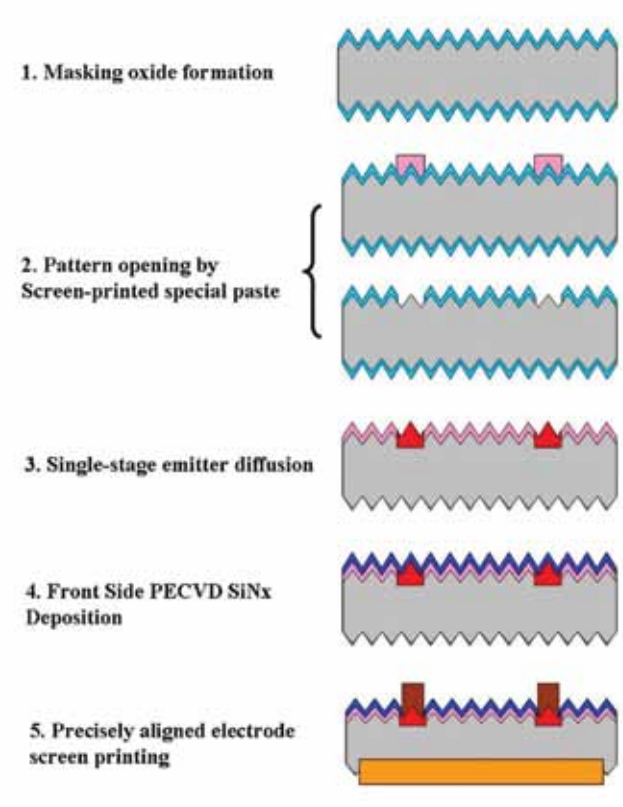

Figure 1. Major processing sequence for manufacture of 6"×6" mc-Si selective-emitter solar cells.

Experimental

The starting substrates are 6"×6", 200µm-thick industrial p-type multicrystalline silicon wafers with a resistivity of 0.5-2Ωcm from Sino-American Silicon Products, Inc. Silicon wafers were first chemically cleaned and acid-etched to remove the saw damage and randomly textured in an HF-HNO_3-H_2O etching solution. An effective light doping zone was formed in the finger region to reduce recombination under the metal contact. The process sequence includes a single diffusion step and used a thermally-grown SiO_2 layer as a mask. An etching paste was then screen-printed to open the oxide barrier for the heavier doping region. After printing the etching paste, the wafers were cleaned in deionized water at room temperature. It is important that the removal of the etching paste is completed thoroughly. The measured line width after etching is about 350µm, while the open region was wider than the Ag-printed finger, which is about 110µm wide.

The dry oxide served as a partial diffusion barrier in order to perform the selective-emitter process with a single diffusion step. The sheet resistance was measured to control the diffusion through the oxide layer. To make a uniform diffusion, several oxide thicknesses were tested and various diffusion processes were performed. The emitter sheet resistances were tested in the range from 40Ω/sq to 120Ω/sq. The reference cells receive a standard homogeneous type emitter with a sheet resistance of 65Ω/sq and 75Ω/sq for mono- and multicrystalline solar cells,

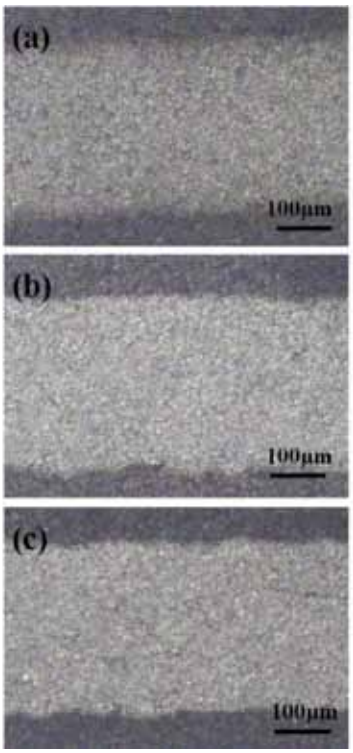

Figure 2. Optical microscopy images of the grid-line opening's coverage of etching paste on the masked oxide layer after (a) 30 seconds, (b) 60 seconds, and (c) 90 seconds of rinsing with deionized water.

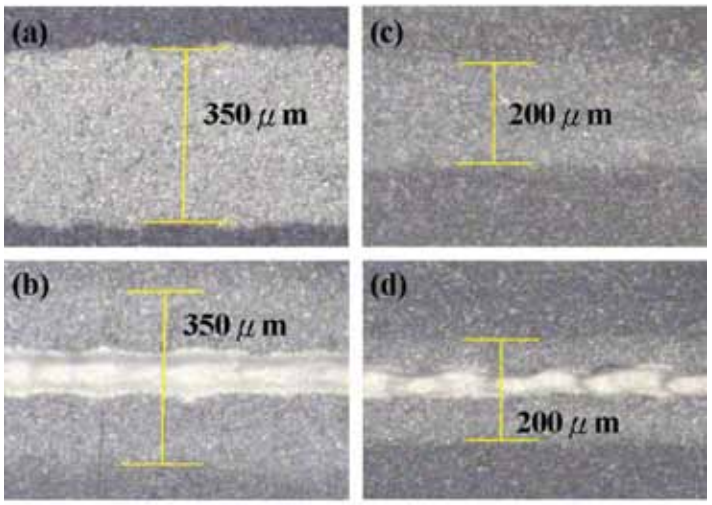

Figure 3. Optical microscopy images of (a) 350μm-wide opening of the masked oxide layer; (b) precise alignment of the electrode finger within the 350μm-wide opening of the masked oxide layer; (c) 200μm-wide opening of the masked oxide layer; (d) precise alignment of the electrode finger within the 200μm-wide opening of the masked oxide layer.

respectively. The emitter sheet resistance of the diffused emitters was measured by the four-point probe technique after the removal of the oxide in a diluted hydrofluoric acid.

The metallization was performed by screen-printing with a precisely-aligned technique and followed by co-firing using an optimized process in a lamp-heated IR belt furnace. This process resulted in simultaneous formation of an Al back-surface field (BSF) and the front Ag grid metallization. Contact patterns for the front side were carried out using a commercial paste from DuPont. The major procedures sequence for this work is shown in Fig. 1.

This study employed light beam-induced current (LBIC) and Corescan measurements to examine the finished solar cells in more detail. The Corescan is a tool developed for detailed surface mapping of the contact resistance between the emitter and the metallization grid of solar cells, while the LBIC scans the continuous wavelength of the Corescan instrument. Owing to the fact that the light used is generated by a halogen lamp, the wavelengths are relatively long and penetrate deeply. Therefore, the LBIC scan method of the Corescan mainly shows the difference in bulk lifetime over the cell. Additionally, contactless microwave-detected photoconductivity decay (μ-PCD) was used to measure the effective lifetime of the samples in this study. Spectral response and reflectance measurements were performed on the fabricated solar cells to determine the quantum efficiency (QE). Current-voltage measurements were taken under a Berger solar simulator using AM1.5 spectrum. The solar cells were kept at 25°C throughout the testing stage.

Heavy/light doping level (Ω/sq)		J_{sc} (mA/cm^2)	V_{oc} (V)	FF (%)	Eff. (%)
40/80	Average	34.36	0.619	77.43	16.46
	STD	0.24	0.006	0.31	0.28
40/100	Average	34.39	0.619	76.82	16.36
	STD	0.19	0.003	0.32	0.22
60/100	Average	34.36	0.618	76.89	16.33
	STD	0.18	0.004	0.52	0.30
60/120	Average	34.59	0.619	76.78	16.43
	STD	0.13	0.006	0.81	0.37
Reference (40Ω/sq)	Average	33.21	0.610	77.85	15.78
	STD	0.49	0.005	0.27	0.39
Reference (70Ω/sq)	Average	34.37	0.616	76.77	16.26

Table 1. The performance of large-volume 6" mc-Si selective emitter solar cells with differing heavy/light sheet-resistance combinations. In this example, 60/100 represents diffusion which reached 60Ω/sq without oxide and 100Ω/sq through the oxide for a certain oxidation time.

Results and discussion

In this study, thermally-grown oxides were used as a partial diffusion barrier to form the selective emitter with a single diffusion step. Dry oxidation was carried out in a tube furnace at temperatures below 900°C. The lower temperature oxidation process is suitable for use with multicrystalline silicon and does not degrade minority carrier lifetime. In the meantime, the accompanied gettering effects maintain the high quality of surface passivation. In general, the application of processes with temperatures higher than ~900°C to solar-grade mc-Si usually leads to a drastic degradation of minority carrier lifetime. An etching paste was screen-printed to open the oxide barrier for heavier doping region. This removal process was done by screen-printing the etching paste on selected areas of the masked oxide layer. Immediately after the etching step, the wafers were rinsed with deionized water for cleaning. Figs. 2(a-c) show optical microscopy images of the opening after 30 seconds, 60 seconds and 90 seconds of deionized water washing, respectively. It was found that 30 seconds' rinsing is not sufficient for cleaning, as some samples still showed traces of the etching paste. Care must be taken during this cleaning

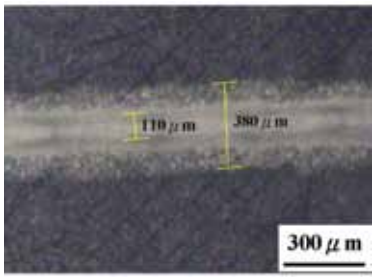

Figure 4. Optical microscopy image showing a typical precise alignment of the electrode finger within the opening of the masked oxide layer. The opened region is 380μm and the silver finger is 110μm wide.

step to ensure prevention of this residual etching paste. The cleaning time was increased and the process was optimized to a stage where the etching paste could be completely removed. In this study, various opening line-widths were also tested (see Fig. 3); however, this study concluded that the opening line-width is not a crucial issue due to the use of higher emitter sheet resistance in the opening regions.

After the single-step $POCl_3$ diffusion, Ag fingers were printed onto the heavier-doped emitter regions. Samples were observed under an optical microscope to check for correct alignment. A typical optical microscopy image, as shown in Fig. 4, reveals the precise result of the alignment between the etched regions and the Ag grids. The open region was wider than the Ag-printed finger, which is approximately 110μm wide.

To ensure a uniform diffusion, several oxide thicknesses were tested and various diffusion processes were performed. The sheet resistance was measured to control the diffusion through the oxide layer. The emitter sheet resistances were tested in the range from 40Ω/sq to 120Ω/sq. Table 1 compares the characteristics of large-volume 6" mc-Si selective emitter solar cells with different heavy/light sheet-resistance combinations. The results listed in Table 1 suggest that the difference between the sheet resistances of the heavy doping (underneath the electrode grid) and the light doping (between the grids) affects the performance of the selective-emitter solar cells.

In this study, the emitter sheet resistances were tested in the range from 40Ω/sq to 120Ω/sq. Many sheet resistance combinations were tested. A compromise must be made between low recombination and low contact resistance. Phosphorus-diffused emitters with a high sheet resistance contribute only marginally to recombination. Table 2 compares the characteristics of the best batch of 6" selective emitter solar cells with modern homogeneous solar cells. The reference cells receive a standard homogeneous type emitter with a sheet resistance of 65Ω/sq and 75Ω/sq for mono- and multicrystalline solar cells, respectively. In comparison to the control mc-Si solar cells with uniformly-doped 70Ω/sq emitter, the mc-Si selective-emitter solar cells with 75/110(Ω/sq)/(Ω/sq) sheet-resistance combination show an

		I_{sc} (A)	V_{oc} (V)	FF (%)	Eff. (%)
c-Si	SE (65/105)	8.995	0.630	78.13	18.22
	Reference (65Ω/sq)	8.946	0.624	77.53	17.82
mc-Si	SE (75/110)	8.527	0.624	77.98	17.07
	Reference (70Ω/sq)	8.438	0.617	77.52	16.62

Table 2. The average efficiency for multi- and monocrystalline selective-emitter solar cells is 17.07% and 18.22%, respectively. Here, 75/110 represents diffusion which reached 75Ω/sq without oxide and 110Ω/sq through the oxide for a certain oxidation time.

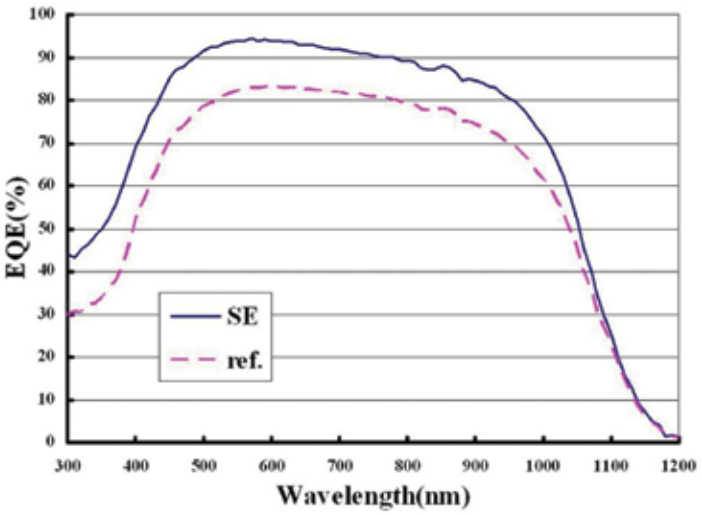

Figure 5. External quantum efficiency (EQE) response for both selective-emitter and conventional uniform-doped emitter solar cells.

average efficiency improvement of more than 0.4% absolute (in this case, 75/110 represents diffusion which reached 75Ω/sq without oxide and 110Ω/sq through the oxide for a certain oxidation time).

Similarly, in comparison to the control c-Si solar cells with uniform doping of 65Ω/sq emitter, the c-Si selective-emitter solar cells with 65/105 (Ω/sq)/(Ω/sq) sheet-resistance combination also show an average efficiency improvement of more than 0.4% absolute. The efficiency of SE cells is significantly higher for both mono- and multicrystalline solar cells.

As shown in Table 2, an improvement of about 7mV on the open circuit voltage (V_{oc}), ~0.4%-0.6% on the fill factor (FF) and about 50-100mA on the short circuit current (I_{sc}) was achieved with the SE cells compared to their homogeneous emitter counterparts. It was found that the recombination under metal contacts affects the performance of the solar cells. This work found that even though the selective-emitter samples suffer from a higher contact resistance, selective-emitter solar cells still show a better overall performance over conventional solar cells. The average contact resistances were 27mΩ/cm^2 and 13mΩ/cm^2 for selective-emitter and conventional cells, respectively. In Table 2, the increase in V_{oc} of selective-emitter cells may be primarily due to lower surface recombination as well as lower Auger recombination, as illustrated in the QE measurement results depicted in Fig. 5. The graph in Fig. 5 displays the QE as a function of the wavelength, and suggests that selective-emitter cells have a higher QE at wavelengths less than 1000nm due to the bulk and front-surface passivation.

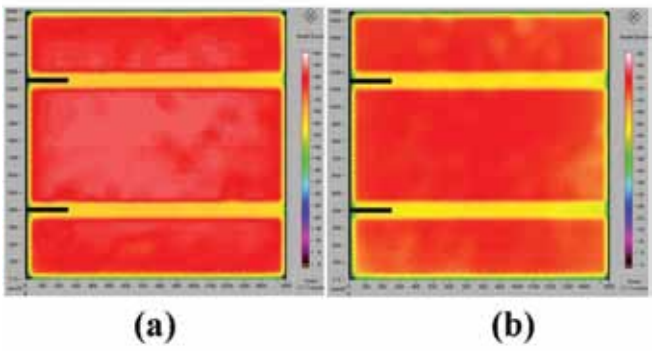

Figure 6. Light beam-induced current (LBIC) maps for: (a) selective-emitter mc-Si solar cells, (b) mc-Si solar cells with a conventional uniform-doped emitter structure. The LBIC is a scan of a continuous-wavelength light beam conducted by the Corescan instrument.

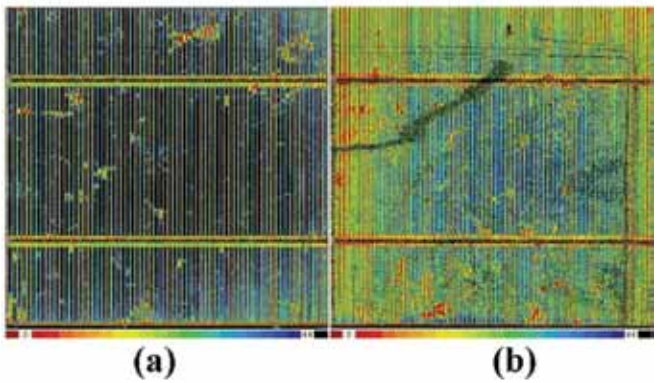

Figure 7. Photoconductance-decay (μ-PCD) maps for: (a) selective-emitter mc-Si solar cells, (b) mc-Si solar cells with a conventional uniformed-doped emitter structure.

> "Even though the selective-emitter samples suffer from a higher contact resistance, selective-emitter solar cells."

I-V and QE results were further supported by light-beam induced current (LBIC) and lifetime measurements. The LBIC scan method is scanning of a light beam over the solar cell while measuring the resulting short-circuit current for each position. Since the LBIC scan method of the Corescan mainly shows the difference in bulk lifetime over the cell, it is clear that the selective-emitter samples fabricated in this work have higher induced current compared to those of conventional solar cells (see Fig. 6). Lifetime mapping also reveals a similar pattern. Fig. 7 shows μ-PCD lifetime mapping after solar cell fabrication.

This study demonstrates that the selective-emitter approach is still an attractive technique even in light/light sheet-resistance combination. The results show that selective-emitter solar cells can have a significant efficiency enhancement over modern solar cells with a uniform lightly-doped emitter. In comparison to mc-Si solar cells with a uniformly-doped 70Ω/sq emitter, an efficiency improvement of more than 0.4% absolute is achieved in large-scale production for selective-emitter solar cells. In this work, the average efficiency for multi- and single-crystalline selective-emitter solar cells is 17.07% and 18.22%, respectively.

Conclusions

The use of low sheet-resistance emitters in conventional multicrystalline silicon solar cells usually results in poor short-

wavelength response. Heavy doping will increase Auger recombination in the emitter region and make effective surface passivation difficult. On the other hand, good quality Ohmic contact to high sheet-resistance emitters is not easy to achieve using normal commercial Ag pastes. These difficulties have focused research efforts on the selective-emitter technique for decades. A selective emitter is a doping layer that is heavily doped beneath the electrode while lightly doped in between the electrode grids. A successful industry implementation of the selective-emitter technique must be capable of displaying a significant efficiency enhancement over modern solar cells with uniform lightly-doped emitters.

The purpose of this study was to develop low-cost multicrystalline selective-emitter silicon solar cells through an optimized single diffusion step, which was achieved by screen-printing etching paste followed by screen-printing precisely-aligned normal Ag paste. The performance of the resultant selective-emitter solar cells was presented and discussed in relation to the different heavy/light sheet-resistance combinations. The results of this work suggest that the difference of sheet-resistance in between heavy doping (underneath the electrode grid) and light doping (in region between the grids) affect the performance of the selective-emitter solar cells. An efficiency improvement of more than 0.4% absolute is achievable for selective-emitter solar cells manufactured using this procedure, resulting in an average efficiency for multi- and monocrystalline selective-emitter solar cells of 17.07% and 18.22%, respectively.

Acknowledgement

The authors would like to thank the support of the Bureau of Energy and the Ministry of Economic Affairs (MOEA).

References

[1] Bultman, J.H. et al. 2006, "Ideal single diffusion step selective emitters: a comparison between theory and practice", *Proc. 16th EU PVSEC*, Glasgow, Scotland, pp.1424-1426.

[2] Ferrada, P. et al. 2009, "Diffusion through semitransparent barriers on p-type silicon wafers", *Proc. 24th EU PVSEC*, Hamburg, Germany, pp. 1897-1900.

[3] Urrejola, E. et al. 2009, "$POCl_3$ diffusion with in-situ SiO_2 barrier for selective emitter multicrystalline solar grade silicon solar cells", *Proc. 24th EU PVSEC*, Hamburg, Germany, pp. 1835-1837.

[4] King, R.R., Sinton, R.A. & Swanson, R.M. 1990, "Studies of diffused phosphorus emitters: saturation current, surface recombination velocity, and quantum efficiency", *IEEE Transactions on Electron Devices*, Vol. 37, No. 2, pp. 365-371.

[5] Okanovic, M. et al. 2009, "Influence of different laser parameters in laser doping from phosphosilicate glass", *Proc. 24th EU PVSEC*, Hamburg, Germany, pp. 1771-1774.

[6] Eisele, S.J. et al. 2009, "18.9% efficient full area laser doped silicon solar cell", *Appl. Phys. Lett.*, Vol. 95, p. 133501.

[7] Fogarassy, E. et al. 1981, "Silicon solar cells realized by laser induced diffusion of vacuum-deposited Dopants", *J. Appl. Phys.*, Vol. 52, No. 2, pp. 1076-1082.

[8] Sameshima, T., Usuzi, S. & Sekiya, M. 1987, "Laser-induced melting of predeposited impurity doping technique used to fabricate shallow junctions", *J. Appl. Phys.*, Vol. 62, No. 2, pp. 711-713.

[9] Horzel, J. et al. 1997, "A simple processing sequence for selective emitters", *Proc. 26th IEEE PVSC*, pp. 139-142.

[10] Rohatgi, A. et al. 2001, "Self-aligned self-doping selective emitter for screenprinted silicon solar cells", *Proc. 17th IEEE PVSC*, pp. 1307-1310.

[11] Porter, L.M., Teicher, A. & Meier, D.L. 2002, "Phosphorus-doped,silver-based pastes for self-doping ohmic contacts for crystalline silicon solar cells", *Sol. Energy Mater. Sol. Cells*, Vol. 73, pp. 209-219.

About the Authors

Ching-Hsi Lin received a Ph.D. degree in materials science and engineering from University of Utah, U.S.A., in 2002. Dr. Lin is currently working at the Industrial Technology Research Institute, Taiwan.

Chien-Hua Lung received a Ph.D. degree in chemistry from National Taiwan University, Taiwan, in 2002. Dr. Lung works at the Industrial Technology Research Institute, Taiwan.

Yu-Wei Tai received his Ph.D. degree in chemical engineering from National Taiwan University in 2005. He then joined the technology development at Neo Solar Power Corporation, and since 2009 has been working as deputy manager of technology development.

Yang-Fang Chen received his Ph.D. degree in physics from Purdue University, USA, in 1984. Dr. Chen is currently a professor in the National Taiwan University, Taiwan. Since 2007, he has been a technical adviser in Neo Solar Power Corporation, consulting in the field of physics, photovoltaics and thin films.

Wei-Chih Hsu received a Ph.D. degree in materials science and engineering from the National Taiwan University, Taiwan, in 2004. Dr. Hsu is currently working at the Industrial Technology Research Institute, Taiwan.

Enquiries

Ching-Hsi Lin,
Rm 402, Bldg. 78, 195, Sec. 4,
Chung Hsing Rd., Chutung, Hsinchu,
Taiwan 310, R.O.C.
Tel: +886 35913358
Email: chinglin@itri.org.tw

Yang-Fang Chen,
No. 1, Sec. 4, Roosevelt Rd., Taipei,
Taiwan 300, R.O.C.
Tel: +886 233665125
Email: yfchen@phys.ntu.edu.tw

Yu-Wei Tai,
7, Li-Hsin 3rd Rd., Hsinchu Science Park,
Hsinchu, Taiwan 300, R.O.C.
Tel: +886 35780011
Email: davidtai@neosolarpower.com